iScience

CellPress
OPEN ACCESS

Article

Lactate-driven type I collagen deposition facilitates cancer stem cell-like phenotype of head and neck squamous cell carcinoma

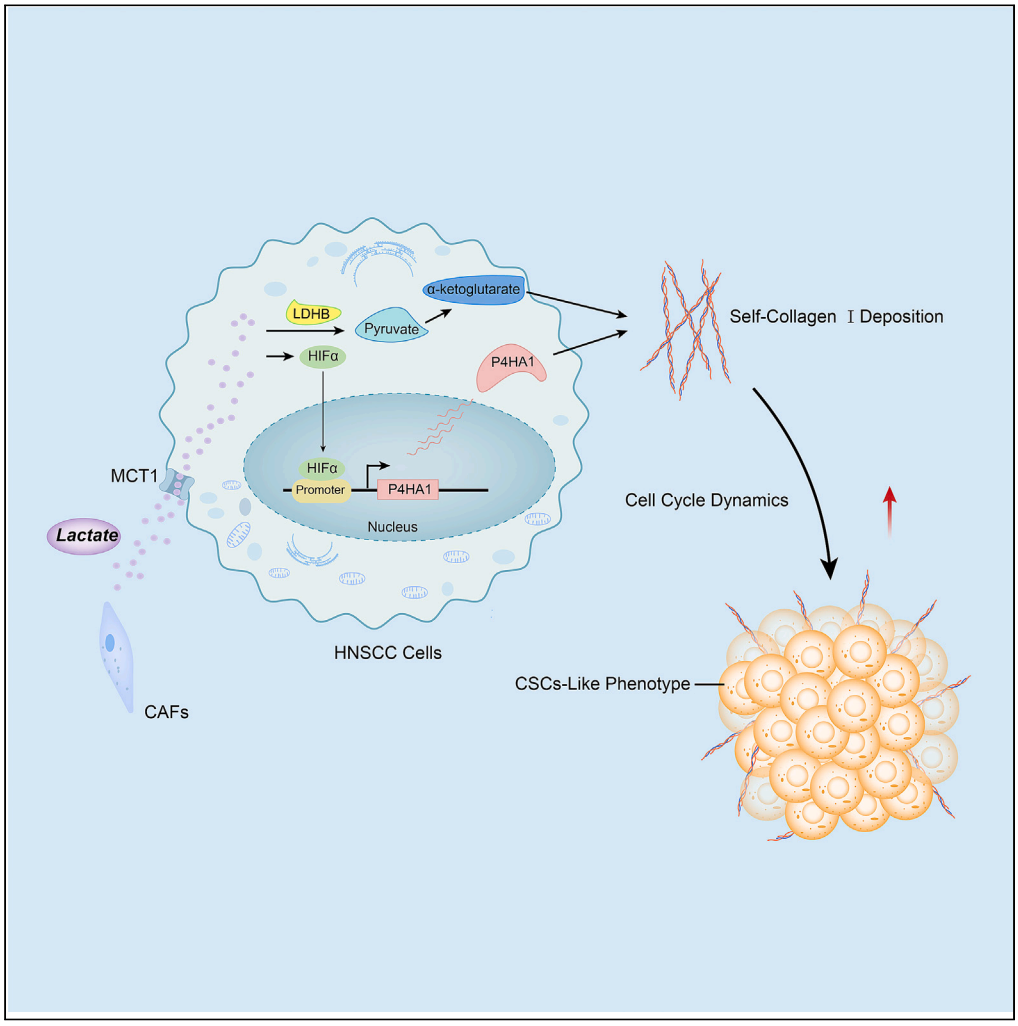

Yunqing Sun, Yang Chen, Hui Zhao, ..., Junqiang Bai, Chuanyu Hu, Zhengjun Shang

chuanyuhu@hust.edu.cn (C.H.)
shangzhengjun@whu.edu.cn (Z.S.)

Highlights

Lactate-driven collagen deposition affects CSCs-like phenotype of HNSCC

Lactate affects collagen by substrate supply and HIF-1α/P4HA1 pathway stimulation

The effect of collagen on CSCs-like phenotype is realized through the cell cycle

Sun et al., iScience 27, 109340
April 19, 2024
https://doi.org/10.1016/j.isci.2024.109340

iScience

CellPress
OPEN ACCESS

Article

Lactate-driven type I collagen deposition facilitates cancer stem cell-like phenotype of head and neck squamous cell carcinoma

Yunqing Sun,[1,7] Yang Chen,[1,3,7] Hui Zhao,[1,2] Jingjing Wang,[1] Yuantong Liu,[1] Junqiang Bai,[1] Chuanyu Hu,[4,5,6,*] and Zhengjun Shang[1,2,8,*]

SUMMARY

Lactate is known to play a crucial role in the progression of malignancies. However, its mechanism in regulating the malignant phenotype of head and neck squamous cell carcinoma (HNSCC) remains unclear. This study found that lactate increases cancer stem cell (CSC) characteristics of HNSCC by influencing the deposition of type I collagen (Col I). Lactate promotes Col I deposition through two distinct pathways. One is to convert lactate to pyruvate, a substrate for Col I hydroxylation. The other is the activation of HIF1-α and P4HA1, the latter being a rate-limiting enzyme for Col I synthesis. Inhibition of these two pathways effectively counteracts lactate-induced enhanced cell stemness. Further studies revealed that Col I affects CSC properties by regulating cell cycle dynamics. In conclusion, our research proposes that lactate-driven Col I deposition is essential for the acquisition of CSC properties, and lactate-centric Col I deposition may be an effective target for CSCs.

INTRODUCTION

Lactate was previously thought to be a metabolic waste product resulting from extensive aerobic glycolysis in tumor cells.[1] However, recent research has revealed that lactate plays multiple roles in shaping the tumor niche, including tumor immune suppression,[2] signaling transduction,[3] and epigenetic modifications.[4,5] Cancer stem cells (CSCs), a minority subpopulation of cells within tumors possessing stem cell-like properties, are crucial in drug resistance and metastasis.[6] Recent scientific findings confirm that CSCs show a preference for uptaking lactate, suggesting that lactate may be essential for maintaining the phenotypic characteristics of CSCs.[7,8] In our previous studies, we demonstrated that lactate, secreted by cancer-associated fibroblasts (CAFs), serves as a substrate for oxidative phosphorylation, enhancing the organoid-forming ability of cancer cells.[9,10] Nevertheless, the mechanism by which lactate regulates the CSC phenotype remains unclear. Identifying the relevance of lactate and CSC properties in head and neck squamous cell carcinoma (HNSCC) is a significant concern that has yet to be elucidated.

Type I collagen (Col I) is the most abundant collagen in the extracellular matrix. It has a tertiary structure composed of two α1 chains and one α2 chain.[11] Several studies have indicated a close correlation between Col I deposition and tumor progression. In breast cancer, lysyl oxidase-mediated Col I deposition can create environments that favor the invasion and metastatic colonization of cancer cells.[12] Additionally, it has been found that non-canonical discoidin domain receptor (DDR) 1 is responsible for promoting lung, bone, and brain metastasis of breast cancer depending on the ubiquitous interstitial Col I.[13] In hepatocellular carcinoma, the activity of collagen type I alpha 1 (COL1A1) confers stronger stemness and enhanced oncogenicity on cancer cells.[14] In colorectal cancer, the binding of Col I and integrin activates the downstream PI3K/AKT/Snail pathway and enhances the CSC properties.[15] Our previous study demonstrates that N-nicotinamide methyltransferase affects the deposition of CAF-derived Col I through epigenetic regulation of LOX, leading to enhanced tumor-initiating frequency and facilitating the formation of tumor organoids.[16] Although the role of Col in manipulating the CSC phenotype has been identified, the underlying mechanism remains unknown. And it also remains unclear whether the environmental lactate is involved in Col I deposition.

[1]State Key Laboratory of Oral & Maxillofacial Reconstruction and Regeneration, Key Laboratory of Oral Biomedicine Ministry of Education, Hubei Key Laboratory of Stomatology, School & Hospital of Stomatology, Wuhan University, Wuhan, China
[2]Department of Oral and Maxillofacial-Head and Neck Oncology, School & Hospital of Stomatology, Wuhan University, Wuhan, China
[3]Department of Oral and Maxillofacial Surgery, School & Hospital of Stomatology, Wuhan University, Wuhan, China
[4]Department of Stomatology, Tongji Hospital, Tongji Medical College, Huazhong University of Science and Technology, Wuhan, China
[5]School of Stomatology, Tongji Medical College, Huazhong University of Science and Technology, Wuhan, China
[6]Hubei Province Key Laboratory of Oral and Maxillofacial Development and Regeneration, Wuhan, China
[7]These authors contributed equally
[8]Lead contact
*Correspondence: chuanyuhu@hust.edu.cn (C.H.), shangzhengjun@whu.edu.cn (Z.S.)
https://doi.org/10.1016/j.isci.2024.109340

COL1A1 contains a significant amount of 4-hydroxyproline, crucial for stabilizing the triple helix structure.[17] Lactate in the tumor microenvironment (TME) can be transported into cancer cells by the monocarboxylate transporter 1 (MCT1) and then converted to pyruvate (PA) for metabolic processes.[9] A recent discovery adds an intriguing layer to this process. Elia et al. find that the environmental PA can assist the tumor cells in shaping the extracellular matrix by hydroxylating Col I. Inhibition of PA metabolism impairs Col I remodeling.[18] Furthermore, lactic acidosis can stabilize hypoxia-inducible factor-1α (HIF-1α) by neutralizing the function of VHL,[19] and HIF-1α is essential for the transcription of prolyl 4-hydroxylase subunit α1 (P4HA1), which is a limiting enzyme in Col I prolyl hydroxylation.[20] These findings suggest that environmental lactate might participate in TME remodeling by affecting Col I deposition. However, the potential mechanism requires further clarification. Therefore, it is imperative to investigate the relationship between lactate and Col I deposition.

In this study, our aim was to elucidate the regulatory mechanism of lactate on the CSC-like phenotype of HNSCC. We confirmed that lactate significantly contributed to the CSC characteristics by enhancing the Col I deposition of tumor cells. On the one hand, lactate served as a metabolic substrate for the α1 chain hydroxylation of Col I through transformation to PA. On the other hand, lactate promoted the hydroxylation and stabilization of Col I by activating the HIF-1α/P4HA1 signaling pathway. Properly processed and hydroxylated Col I could enhance the CSC properties of tumor cells by accelerating the cell cycle dynamics. Our research provided a promising therapeutic approach for targeting CSCs of HNSCC.

RESULTS

Lactate-driven Col I deposition enhances the CSC properties

The lactate in acidic TME widely participates in the immunosuppression, therapeutic resistance, and phenotypic modulation of malignancies.[3] In our previous studies, we demonstrate that CAFs-derived lactate can enhance the organoid-forming ability and promote the progression of oral squamous cell carcinoma.[9,10] However, the role of lactate on CSC phenotype is poorly clarified. Col I, the most abundant protein in TME, is involved in the tumorigenesis, progression, and CSC phenotypic modulation of malignancies.[21–23] Yet, whether the environmental lactate contributes to Col I deposition remains elusive. Here, we found lactate-treated HNSCC cells had increased Col I deposition (Figures 1A and S1A) and elevated COL1A1 expression (Figure 1B). Our previous experiments demonstrated the enhancing effect of lactate on organoid CSC properties.[10] CSCs are a small subpopulation of cancer cells within tumors and have stronger self-renewal and recurrence capacity when compared to non-CSCs.[24] In this study, we found lactate-treated CAL27 and SCC9 cells had increased expression of CSC-related markers (Figure 1C) and possessed higher sphere-initiating frequency (Figure 1E). AZD3965, the MCT1-specific inhibitor, was added to restrict lactate uptake.[25] This limitation caused the disappearance of collagen deposition and CSC properties brought about by lactate (Figures 1B and 1C). The results of flow cytometry also demonstrated an increase in the $CD44^{+}/CD133^{+}$ ratio in response to lactate (Figures 1D, S1B, and S1C). To confirm whether lactate-driven Col I deposition was involved in the regulation of CSC phenotype, the shCOL1A1 and oeCOL1A1 cell lines were constructed (Figures S1D and S1E). We found knockdown of COL1A1 dampened the CSC properties induced by lactate, including downregulation of CSC-related markers and decreased sphere formation and clonogenic abilities, while overexpression COL1A1 or adding exogenous Col I rescued the CSC properties (Figures 1F, 1G, and S1F). Together, the aforementioned results demonstrate that lactate manipulates the CSC properties via promoting the Col I deposition of tumor cells, but the mechanism by which lactate regulates Col I needs to be further clarified.

Lactate boosts Col I deposition partially via transforming to PA

In previous part, we demonstrate the environmental lactate contributes to Col I deposition of tumor cells, thus leading to the enhanced CSC properties. Given this result, we aim to explore the intrinsic mechanism by which lactate modulates Col I deposition in this part. Lactate is transported to cells by MCT1 and then converted to PA by lactate dehydrogenase B (LDHB).[26,27] Recently, researchers found PA can support the extracellular matrix remodeling of cancer cells by hydroxylating Col I.[18] In our research, we found LDHB expression was associated with Col I deposition contributed from lactate (Figure 2A). Exogenous lactate was absorbed by CAL27 and SCC9 cells in 72 h and the expression of intracellular PA ascended to its peak at around 48 h (Figures 2B and 2C). Subsequently, we measured the lactate and pyruvate levels in cells treated with siMCT1 and siLDHB 48 h after lactate treatment. The results revealed that blocking lactate uptake and its conversion to pyruvate restricted the increase in pyruvate levels (Figures S2A and S2B). Besides, LDHB was highly expressed in HNSCC and correlated with poor survival (Figures 2D and 2E). As PA hydroxylates Col I by inducing the production of α-ketoglutarate (AKG),[18] we detected the intracellular AKG at 48 h, and a significantly increased expression of AKG was observed (Figure S2C). To verify our speculation, we targeted lactate uptake by knocking down the lactate transporter MCT1 and lactate metabolism by interfering with the LDHB (Figures S2D and S2E). It was noteworthy that targeting MCT1 completely inhibited lactate-induced Col I deposition and CSC properties, whereas targeting LDHB only partly abolished the effect of lactate (Figures 2F–2J). This indicates that lactate boosts Col I deposition partially via transforming to PA; some of the other unknown pathways may also be involved and need to be further explored.

Lactate promotes Col I deposition partly through the HIF-1α/P4HA1 pathway

Lactate is the "root of all evils" of the acidic TME; previous study reveals that lactic acidosis can stabilize HIF-1α by neutralizing the function of VHL.[19,28] At the protein level, this phenomenon occurs, and the mRNA of HIF-1α remains unchanged despite the addition of lactate (Figure S2F). HIF-1α is involved in various cancer biological behaviors by regulating the transcription of its target genes.[29] In actuality, a study suggests that HIF-1α is essential for the transcription of P4HA1, which is indispensable for proper Col I-propolypeptide chains hydroxylated.[30] Therefore, we wondered whether lactate could promote Col I deposition partly through the HIF-1α/P4HA1 pathway. Here, we found lactate

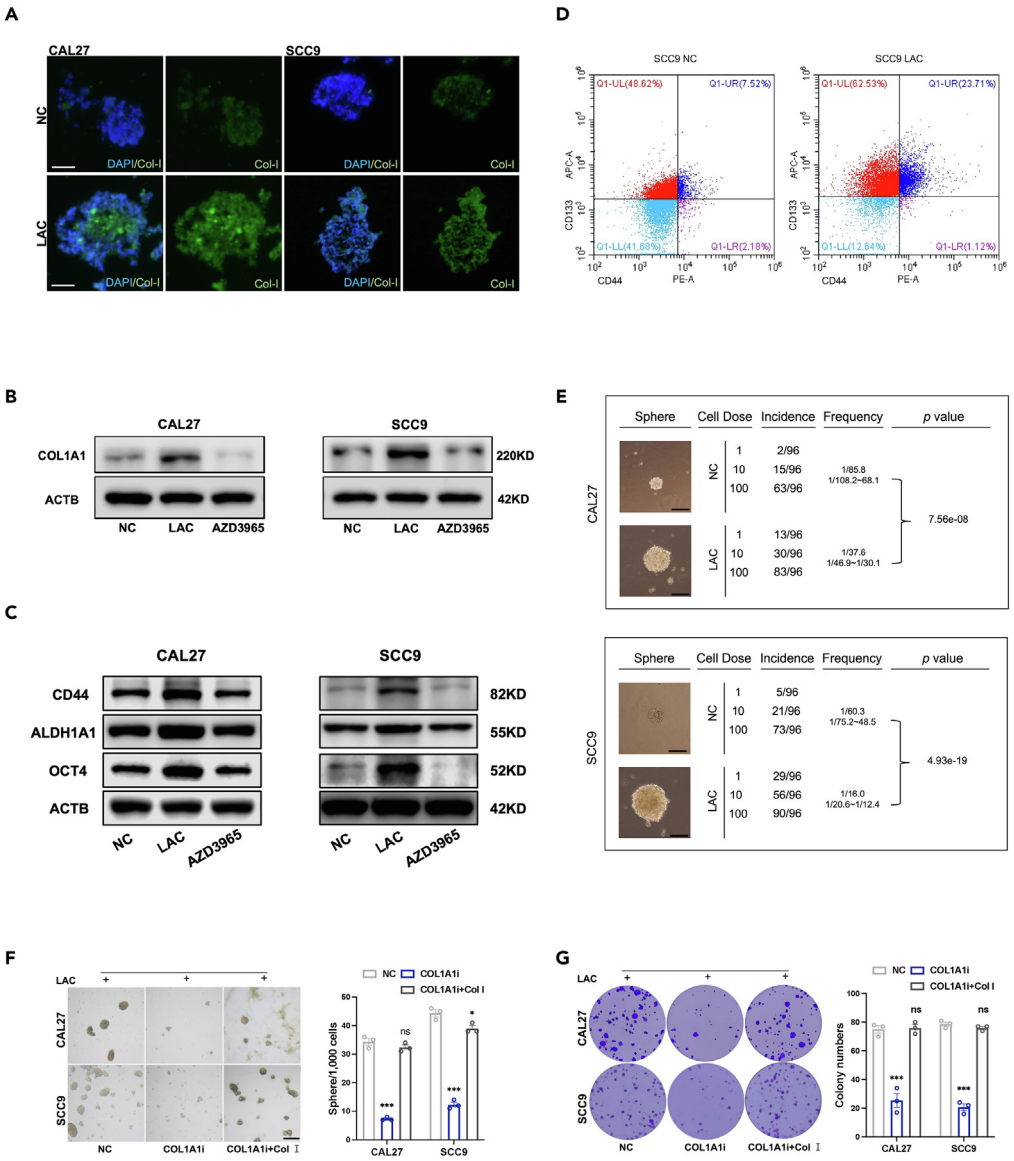

Figure 1. Lactate-driven type I collagen deposition enhances the CSC properties

(A) We used immunofluorescence assay to observe the expression of Col I of spheres in the NC and LAC groups. n = 3, Scale bars, 50 μm.

(B) Western blot was used to detect the expression of COL1A1 in the NC, LAC, and AZD3965 (25 nm) with LAC groups of HNSCC cells.

(C) Western blot was used to detect the expression of CSC-related markers in the NC, LAC, and AZD3965 (25 nm) with LAC groups of HNSCC cells.

(D) Flow cytometry was employed to assess the CSC markers in HNSCC cells before and after lactate treatment, with CD133 labeled with APC staining and CD44 labeled with PE staining (SCC9).

(E) Limiting dilution analysis was performed to determine the sphere-initiating frequency. The ELDA software was used for processing data.

(F and G) Sphere formation assay (F) and clonogenic assay (G) was utilized to examine the stemness and tumorigenesis in the NC (empty vector), COL1A1i and exogenous Col I of two HNSCC cell lines. All groups were treated with lactate. n = 3, Scale bars, 200 μm. Data are presented as means ± SEM. ns, not significant. *p < 0.05, **p < 0.01, ***p < 0.001.

increased the expression of HIF-1α in CAL27 and SCC9 cells (Figures 3A and 3B). To determine the role of HIF-1α/P4HA pathway played in collagen regulation, we constructed the oeP4HA1 cell lines (Figure S3A). And overexpression of P4HA1 rescues the downregulation of COL1A1 caused by siHIF-1α (Figure S3B). Then, we searched the motif of HIF-1α in the JASPAR database (https://jaspar.genereg.net) and predicted its potential binding sites on the promoter of P4HA1 (Figures 3C and 3D). ChIP assay was used to enrich the DNA sequences that were associated with HIF-1α. qPCR was performed to determine if the predicted sites were specifically enriched by immunoprecipitation. And we found that HIF-1α bound to the "CTACGTGA" sequence of the promoter region of P4HA1 and enhanced its transcriptional activity (Figure 3E). Next, we interfered with the expression of HIF-1α and P4HA1 by different siRNAs (Figures S3C and S3D). We found neither

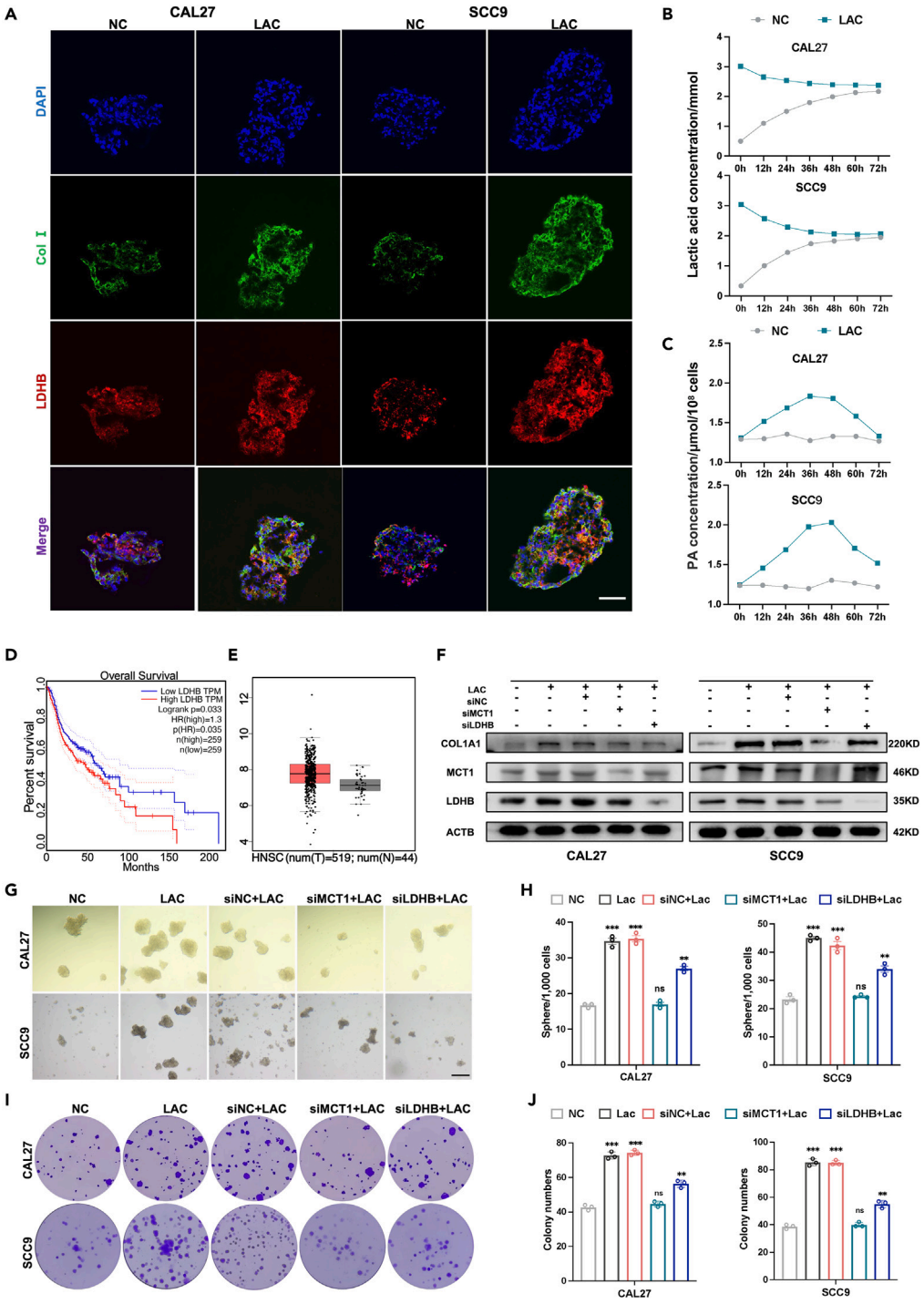

Figure 2. Lactate boosts Col I deposition partially via transforming to PA

(A) Immunofluorescence was used to observe the expression of Col I and LDHB of spheres in the NC and LAC groups. Scale bars, 50 μm.

(B and C) Supernatant lactic acid content (B) and intracellular PA content (C) in the NC and LAC groups of HNSCC cells. n = 3.

(D and E) Survival analysis (D) and expression boxplot (E) of LDHB from GEPIA. (http://gepia.cancer-pku.cn/) (F) Western blot was performed to determine the expression of COL1A1, MCT1, and LDHB of sphere cells in the NC, LAC, siNC+LAC, siMCT1+LAC, and siLDHB+LAC groups.

(G–J) Sphere formation assay (G, H) and clonogenic assay (I, J) was used to determine the stemness and tumorigenesis in the NC, LAC, siNC+LAC, siMCT1+LAC, and siLDHB+LAC groups. n = 3, Scale bars, 200 μm. Data are presented as means ± SEM. ns, not significant. **p < 0.01, and ***p < 0.001.

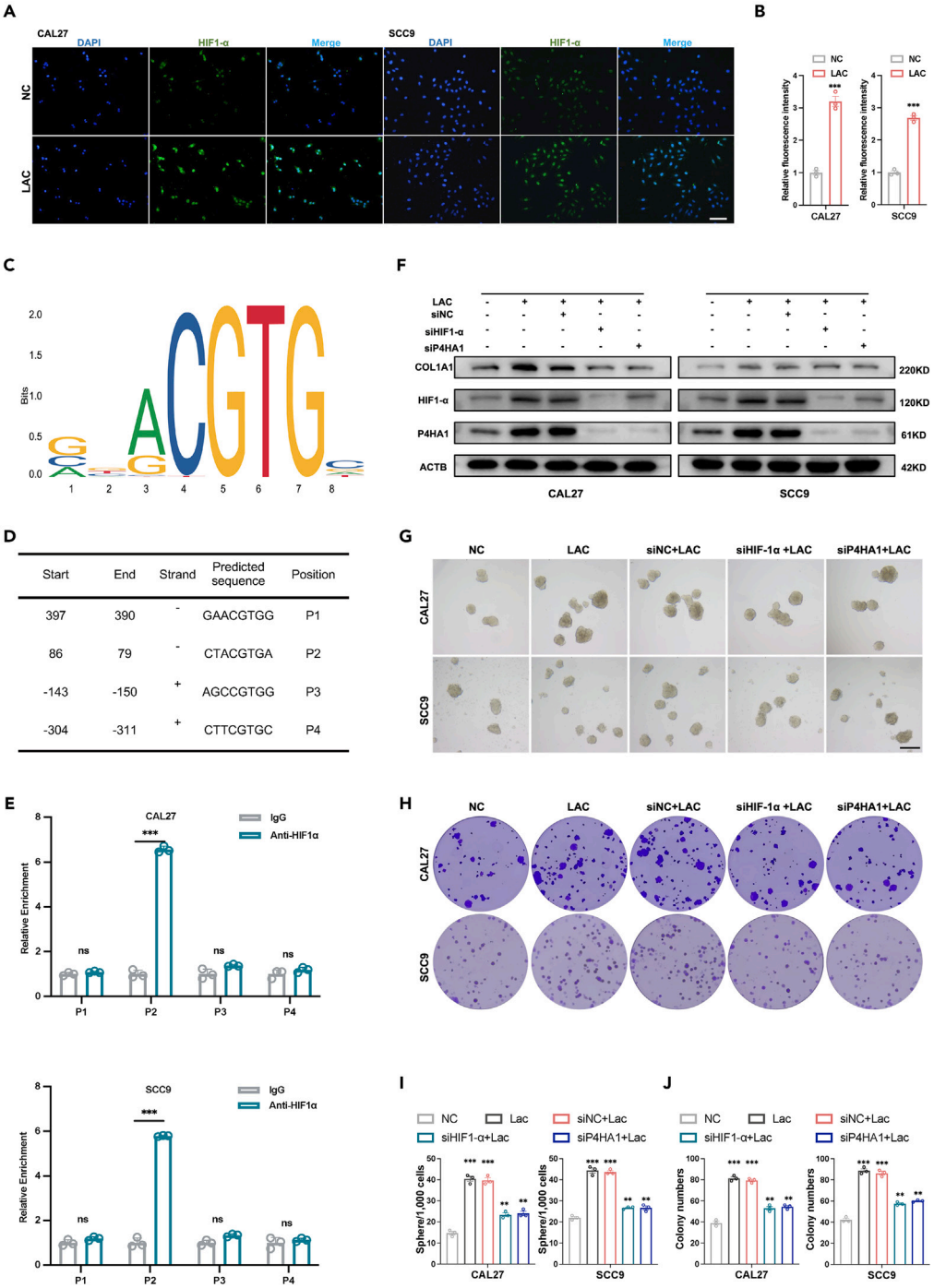

Figure 3. Lactate promotes Col I deposition partly through the HIF-1α/P4HA1 pathway

(A and B) Immunofluorescence was used to observe the content of HIF-1α in the NC and LAC groups (A) representative images and (B) quantification analysis. n = 3, Scale bars, 100 μm.

(C–F) ChIP assay was used to determine the precise binding site of HIF-1α with P4HA1 promoter. The predicted binding motif of HIF-1α (C), predicted binding sequences and positions in P4HA1 promoter (D), and relative enrichment of HIF-1α of each position in P4HA1 promoter (E). n = 3. F Western blot was performed to determine the expression of COL1A1, HIF-1α, and P4HA1 of sphere cells in the NC, LAC, siNC+LAC, siHIF-1α+LAC, and siP4HA1+LAC groups.

(G–J) Sphere formation assay (G, I) and clonogenic assay (H, J) were used to determine the stemness and tumorigenesis in the NC, LAC, siNC+LAC, siHIF-1α+LAC, and siP4HA1+LAC groups. n = 3, Scale bars, 200 μm. Data are presented as means ± SEM. ns, not significant. **p < 0.01, ***p < 0.001.

knockdown of HIF-1α nor P4HA1 could completely block lactate-induced Col I deposition as well as the sphere formation and clonogenic abilities (Figures 3F–3J). In conclusion, these results demonstrate that lactate promotes Col I deposition partly through the HIF-1α/P4HA1 pathway.

Col I enhances CSC properties through regulating cell cycle dynamics

To clarify the mechanism by which Col I regulates the CSC properties, we treated the NC (empty vector) and COL1A1i cells with lactate and sequenced their transcriptome. 7,894 differentially expressed genes (DEGs) were obtained, including 4,646 upregulated genes and 3,248 downregulated genes (Figures 4A and 4B). The gene ontology (GO) and Kyoto Encyclopedia of Genes and Genomes (KEGG) pathway analysis of the 3,248 downregulated DEGs were performed, and we found knockdown of COL1A1 affected the DNA replication, nuclear division, and chromosome-related pathway by GO analysis (Figure 4C). To achieve a deeper enrichment, we conducted a study of the downregulated pathways in the KEGG analysis, and the cell cycle process emerged as the most correlated and differential one (Figure 4D). As the cell cycle is mechanistically linked to the self-renewal, pluripotency, and cell fate of stem cells,[31] we wondered whether Col I regulates CSC properties through cell cycle dynamics. At first, we found knockdown of COL1A1 decreased the number of proliferative cells and increased the proportion of cells in the G1 phase (Figures 4G and S4A). The decreased expression of pRB, CyclinE1, and Cyclin D1 and elevated expression of p21 were also observed and rescued by exogenous collagen addition (Figure 4H). These results confirmed that knockdown of COL1A1 could cause cell-cycle arrest in HNSCC cells. Then, overexpression of COL1A1 resulted in an elevation of CSC markers in tumor cells (Figure 4I). However, the cell cycle inhibitor palbociclib mitigated the effects induced by COL1A1 without affecting COL1A1 expression itself. All in all, these results verify that lactate-driven Col I can orchestra CSC properties by regulating cell cycle dynamics.

Simultaneously targeting LDHB and HIF-1α interdict lactate-induced Col I deposition and CSC properties

As both LDHB and HIF-1α are involved in lactate-induced Col I deposition and CSC properties, we concurrently interfered with the expression of LDHB and HIF-1α. The results showed simultaneously targeting LDHB and HIF-1α thoroughly blocked lactate-induced CSC properties (Figures 5A, 5B, and S4B). Besides, the enhanced CSC-like phenotype caused by lactate, such as elevated sphere formation and clonogenic capacities, was deprived (Figures 5B, 5C, and 5E). However, adding exogenous Col I restored the CSC properties of HNSCC cells (Figures 5B, 5C, and 5E). To determine the roles of lactate *in vivo*, lentivirus-infected CAL27 cells were constructed (Figure S4C) and injected subcutaneously in mice. Lactate and Col I were injected into the tumor region every 3 days. As expected, lactate enhanced the tumorigenicity of HNSCC. Treatment with lactate increased the volume and weight of tumors (Figure 6C). The lactate group also had elevated CD44, ALDH1A1, pRB expression, and Col I deposition (Figures 6D and 6E). Consistent with the *in vitro* studies, simultaneously targeting LDHB and HIF-1α blocked lactate-enhanced Col I deposition and tumorigenicity, but treatment with Col I rescued the dampened tumorigenic ability (Figures 6A and 6B). Overall, we verify both PA and HIF-1α/P4HA1 participate in lactate-derived Col I deposition, simultaneously targeting LDHB and HIF-1α that block lactate-induced Col I deposition and CSC properties.

DISCUSSION

Cancer is a malignant disease that poses a serious threat to human health and is currently incurable.[32] Metastasis and recurrence of advanced tumors are the major challenges confronted in treatment, wherein CSCs play a pivotal role.[33,34] CSCs possess unique biological properties and metabolic patterns. Thus, targeting CSCs has been proven to improve therapeutic outcomes and lead to a better prognosis.[35–37] In this research, we validate that lactate promotes deposition of Col I through both the PA and HIF-1α/P4HA1 pathways. The lactate-derived Col I is essential for maintaining the CSC phenotype in HNSCC (Figure 7).

Recent studies have revealed that aerobic glycolysism, an inefficient but fast energy-supplying metabolic pathway, predominantly occurs during the tumor rapid progress period.[38] CAFs in TME secrete more lactate,[9,10] subsequently taken up by cancer cells as a substrate for oxidative phosphorylation and biosynthesis.[39] Our previous studies have revealed that CAFs-derived lactate is critical for the self-renewal and progression of oral squamous cell carcinoma.[9,10] However, the mechanism underlying lactate regulation on CSC phenotype has not been elucidated. In this research, we treated HNSCC with exogenous lactate as a substitute for CAFs-derived lactate. Our observations revealed that lactate promoted the proliferation, invasion, and migration of cancer cells, enhancing their CSC properties. Col I, an indispensable component of extracellular matrix (ECM),[22] plays a role in the progression of multiple malignancies, including HNSCC,[40] breast cancer,[41] lung adenocarcinoma,[42] pancreatic cancer,[43] and colorectal cancer.[44] However, the impact of environmental lactate on CSC properties by promoting Col I deposition remains unclear. Here, we reveal that lactate can be transported to HNSCC cells by MCT1, and then converted to PA by LDHB. PA further provided a substrate for proline hydroxylation of COL1A1 by transforming to AKG. Meanwhile, lactate inhibited the degradation of HIF-1α, which could bind to the promoter region of P4HA1 and enhance its transcriptional activity, thus accelerating the proline hydroxylation of COL1A1. Recently, Elia et al. find the crucial role of environmental PA in ECM remodeling by hydroxylating Col I; inhibition of PA metabolism impairs Col I remodeling.[18] Besides, lactate can stabilize HIF-1α by neutralizing the function of VHL,[19] and HIF-1α is essential for the transcription of P4HA1. Based on the previous studies, we further validate the effect of lactate on regulation of the Col I deposition, and confirm simultaneously targeting LDHB and HIF-1α blocks lactate-induced Col I deposition and CSC properties.

Col I drives epithelial-mesenchymal transition and increases invasive propensity in pancreatic and breast cancers through activation of DDR1b/SHC1 and DDR2/ERK2 pathways.[41,43] Additionally, Col I binds to integrins, activating the MEK/ERK and Rho-related kinase, thus promoting the malignancy of oral and skin squamous cell carcinomas.[40,45] There is no doubt that Col I can influence tumor progression through

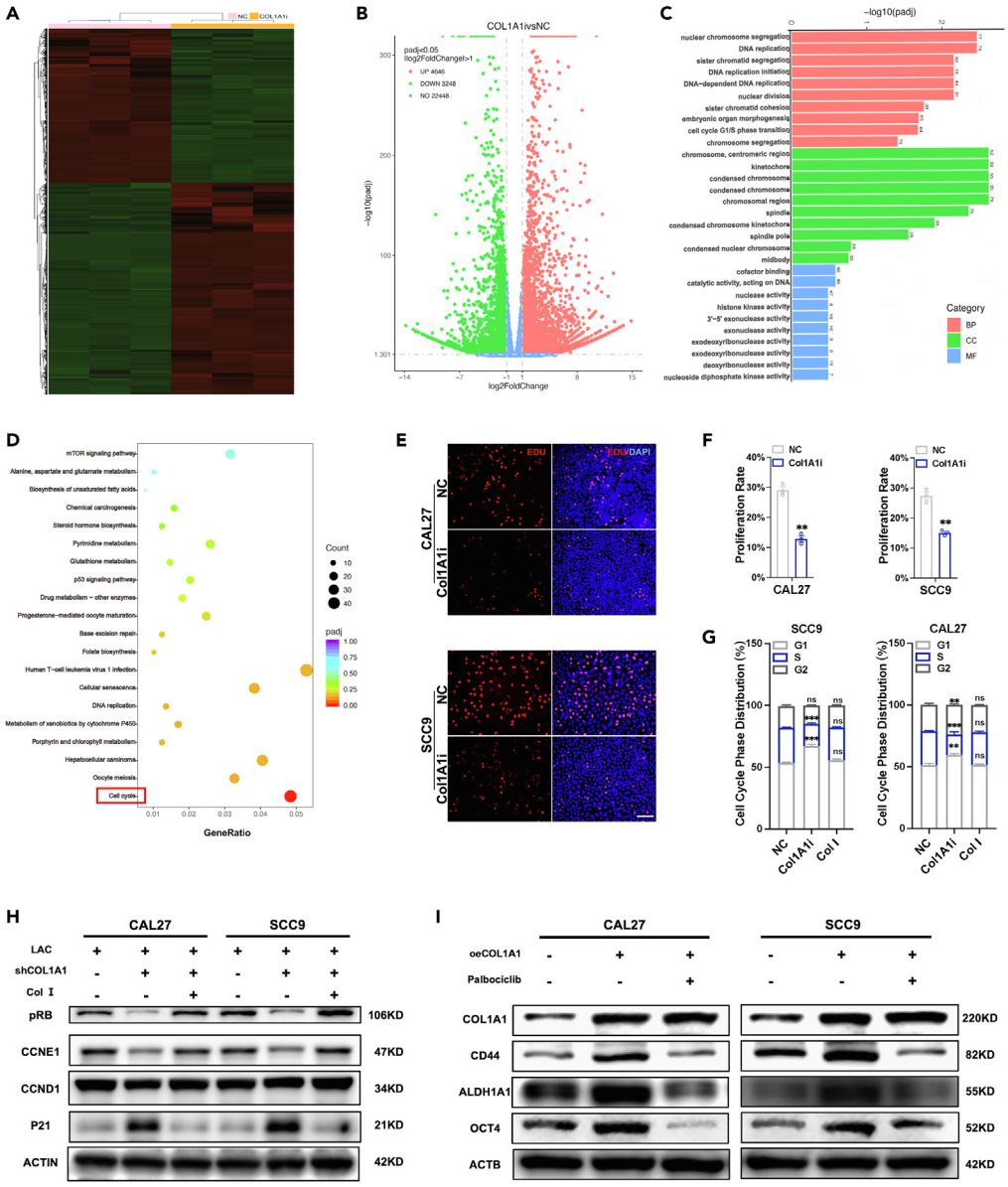

Figure 4. Lactate-driven Col I enhances CSC properties through cell cycle dynamics

(A and B) The heatmap and volcano map of DEGs in the NC and COL1A1i. All groups were treated with lactate.

(C) The GO analysis of all DEGs.

(D) The KEGG pathway analysis of downregulated DEGs.

(E and F) Representative images (E) and quantification analysis (F) of EdU assay showed that COL1A1i reduced the proliferation of HNSCC cells. n = 3, Scale bars, 100 μm.

(G) Quantification analysis of cell cycle analysis (Figure S2E) showed that COL1A1i increase the proportion of HNSCC cells in the G1 phase and exogenous Col I restored the cell cycle dynamics. All groups were treated with lactate. n = 3.

(H) Western blot was used to examine the expression of cell cycle phase markers in the NC, shCOL1A1, and shCOL1A1 with Col I groups. All groups were treated with lactate.

(I) Western blot was conducted to examine the expression of cell CSC markers in the NC, oeCOL1A1, and oeCOL1A1with Palbociclib (500 nm) groups. Data are presented as means ± SEM. ns, not significant. *p < 0.05, **p < 0.01, and ***p < 0.001.

the TME remodeling. However, the mechanism by which Col I supports the CSC phenotype is still poorly understood. One possible mechanism is that Col I may enhance the stemness of cancer cells by activating extracellular signals, including integrins, and DDRs, to stimulate downstream cascades. Another hypothesis is that Col I may regulate the composition and structure of ECM, thereby influencing the signaling and biological behavior of cancer cells. To further elucidate the specific mechanism by which Col I affects the stemness of HNSCC, we

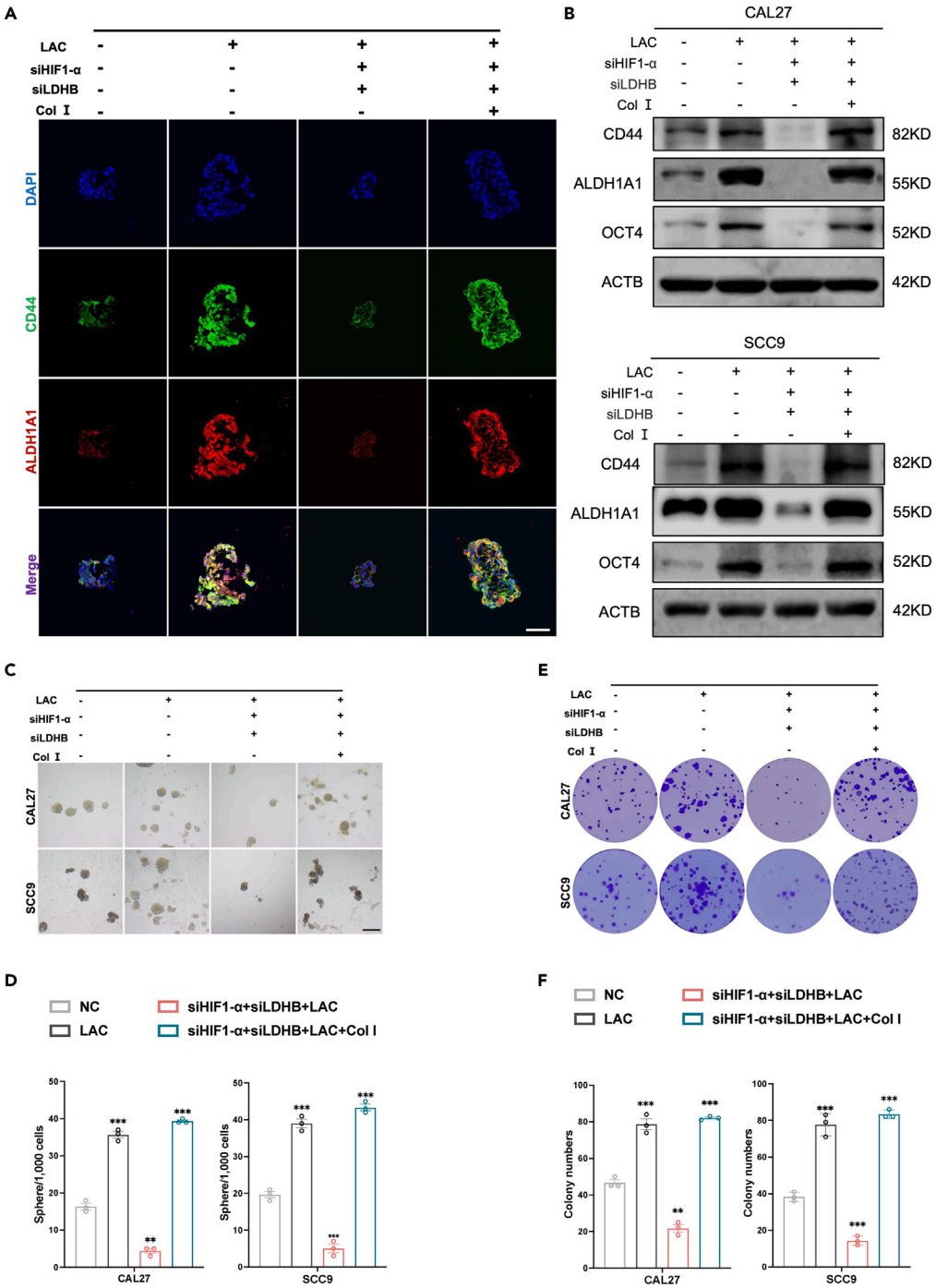

Figure 5. Simultaneously targeting LDHB and HIF-1α interdict lactate-induced stemness of HNSCC cells

(A) Immunofluorescence was used to observe the expression of stemness markers CD44 and ALDH1A1 of spheres in the NC, LAC, LAC+siHIF-1α+siLDHB, and LAC+siHIF-1α+siLDHB+Col I groups. Scale bars, 50 μm.

(B) Western blot was performed to determine the expression of stemness markers CD133, ALDH1A1, OCT4, and BMI1 in the NC, LAC, LAC+siHIF-1α, LAC+siHIF-1α+Col I, LAC+siLDHB, LAC+siLDHB+Col I, LAC+siHIF-1α+siLDHB, and LAC+siHIF-1α+siLDHB+Col I groups.

(C–F) Sphere formation assay (C, D) and clonogenic assay (E, F) were used to determine the stemness and tumorigenesis of the NC, LAC, LAC+siHIF-1α+siLDHB, and LAC+siHIF-1α+siLDHB+Col I groups. n = 3, Scale bars, 200 μm. Data are presented as means ± SEM. **p < 0.01, ***p < 0.001.

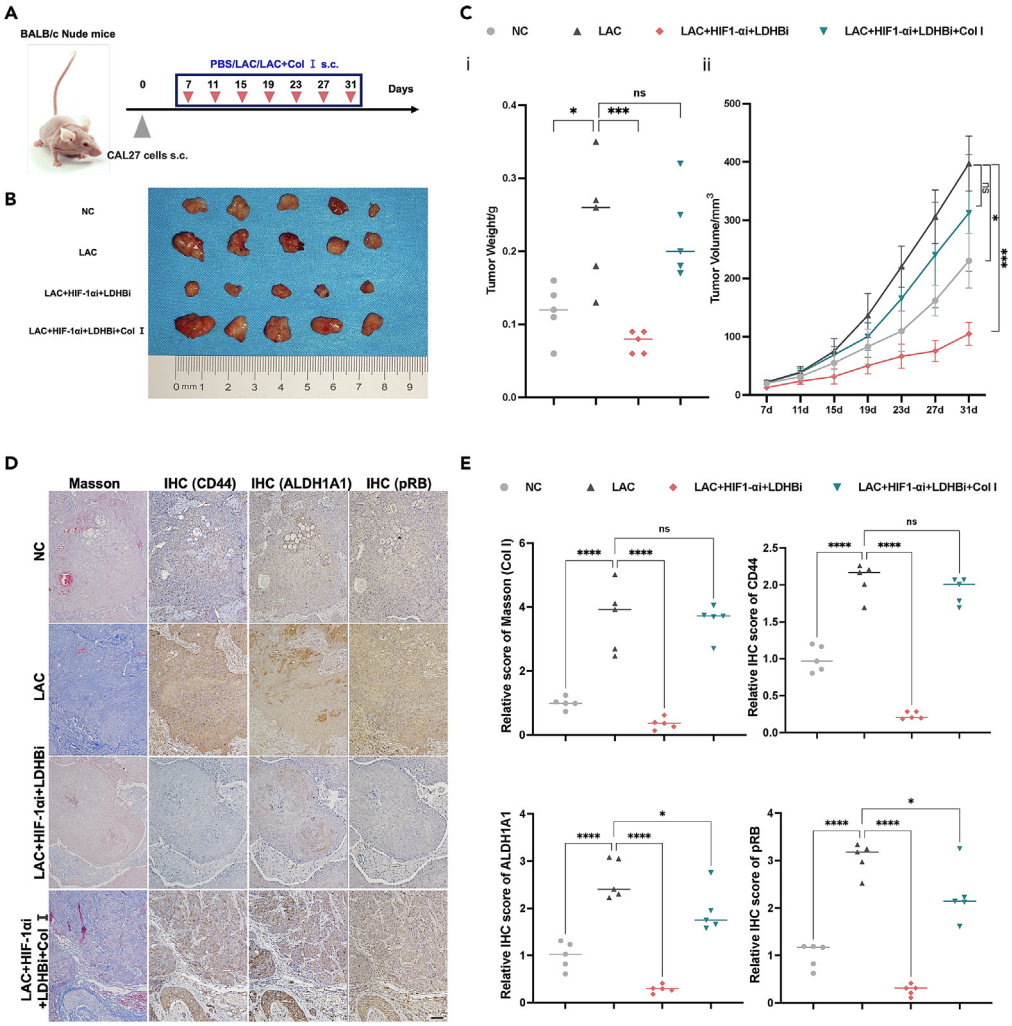

Figure 6. Concurrently interfering LDHB and HIF-1α interdict lactate-induced tumor growth

(A) Schematic diagram of the nude mouse tumor-bearing experiment. BALB/c nude mice were transplanted with CAL27 cells infected with either empty vectors (NC) or lentivirus containing both HIF-1α and LDHB knockdown sequences. Then, the mice were injected with PBS, lactate, or lactate+ Col I every 4 days starting on day 7, depending on the group. 5 rats were assigned to each group. Xenograft tumors were harvested on day 31.

(B) Tumor image of xenograft. n = 5.

(C) Quantification analysis of tumor weight (i) and volume (ii). n = 5.

(D and E) Representative images (D) and quantification analysis (E) of Masson staining of Col I and immunohistochemical staining of CD44, ALDH1A1, and pRB. Data are presented as means ± SEM. ns, not significant. *p < 0.05, ***p < 0.001 and ****p < 0.0001.

performed RNA sequencing after knockdown of Col1A1. Our findings reveal Col I maintains CSC properties by accelerating the cell cycle and self-renewal of cancer cells. This study uncovers a novel mechanism by which Col I affects the phenotype of CSCs, enriching our understanding of the roles of Col I remodeling in the regulation of cancer progression.

In HNSCC, the metabolic patterns of oxidative phosphorylation and aerobic glycolysis coexist and adapt to different environments based on the transformation of metabolic patterns.[46] The tumor's malignancy is robustly supported by the rapid energy supply pathway of glycolysis, as well as enhanced energy supply pathways such as lipid metabolism and protein metabolism during tumor progression and invasion.[47] Additionally, HNSCC can uptake lactate secreted by cancer-CAFs and augment their own oxidative phosphorylation to promote tumorigenesis.[10] The crux of our study is that lactate-mediated collagen deposition promotes the CSC-like phenotype, and our current experimental results are robust enough to support this conclusion. We plan to further explore the interesting question whether CSCs or differentiated cancer cells predominantly consume lactate-mediated collagen deposition in subsequent stages of our research.

In summary, our researches reveal that lactate regulates CSC-like phenotype through pyruvate and HIF-1α/P4HA1-mediated collagen deposition. Lactate-driven Col I deposition is essential for the acquisition of the CSC phenotype. Our study provides valuable insights to

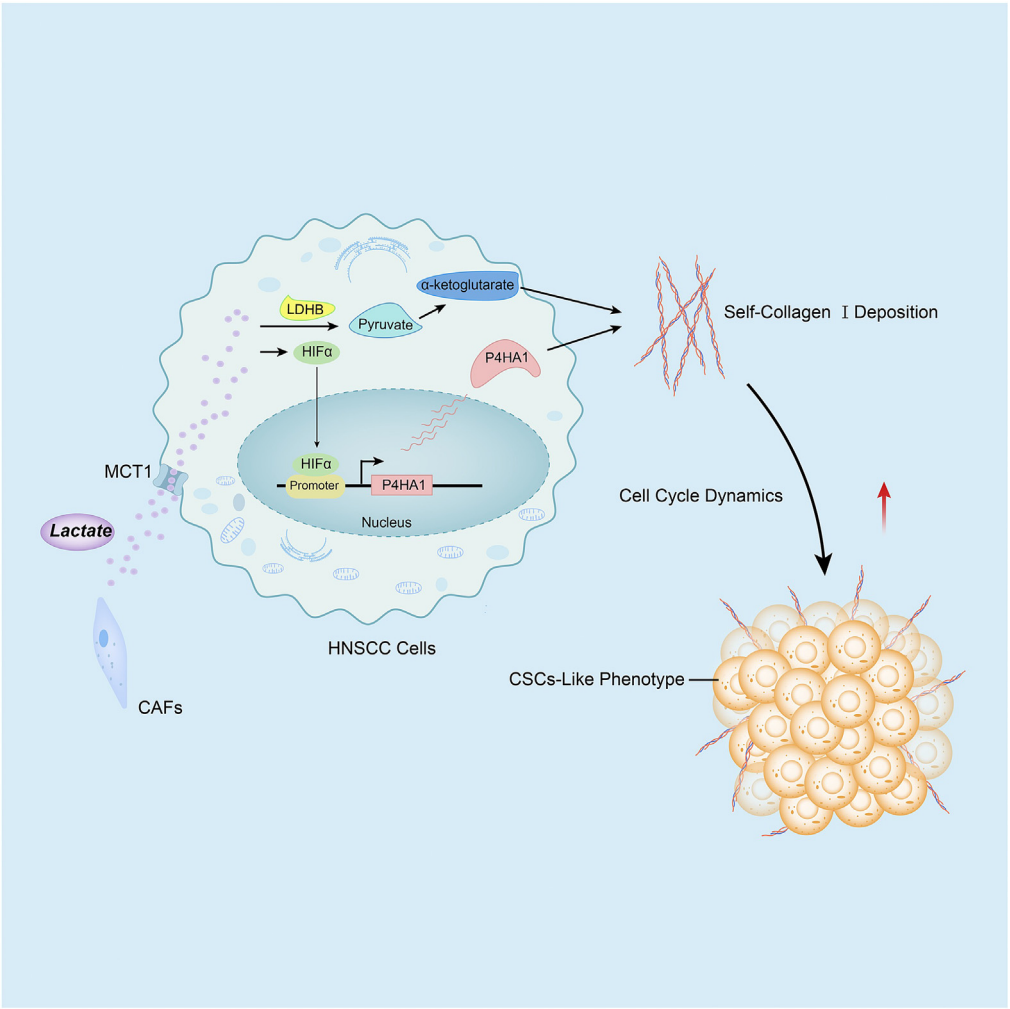

Figure 7. Schematic of the mechanism of lactate in regulating CSCs-like phenotype of HNSCC

The lactate in the tumor microenvironment is transported to cancer cells by MCT1. Then, lactate is converted to pyruvate and α-ketoglutarate, which are substrate for collagen I deposition. In the meantime, lactate activates HIF1α and promotes the transcription of P4HA1, which is a rate-limiting enzyme for collagen I synthesis. Next, the lactate-driven collagen I deposition enhances the CSCs properties of HNSCC cells through accelerating cell cycle dynamics.

explain the formation of small ecological niches in circulating tumor cells during tumor metastasis. Targeting lactate-centric Col I deposition may prove effective in preventing the metastasis of HNSCC.

Limitations of the study

This research was centered on oral squamous cell carcinoma cell lines and established animal models for subcutaneous tumor formation. To advance our investigations, our research team is in the process of developing oral squamous cell carcinoma organoids and *in situ* oral tumor formation. We are eager to enhance result validation by utilizing more sophisticated models that closely resemble living organisms.

STAR★METHODS

Detailed methods are provided in the online version of this paper and include the following:

- KEY RESOURCES TABLE
- RESOURCE AVAILABILITY
  - Lead contact
  - Materials availability
  - Data and code availability
- EXPERIMENTAL MODEL AND STUDY PARTICIPANT DETAILS

SUPPLEMENTAL INFORMATION

Supplemental information can be found online at https://doi.org/10.1016/j.isci.2024.109340.

ACKNOWLEDGMENTS

This study was supported by the National Natural Science Foundation of China (nos. 82273306 and 82002893).

AUTHOR CONTRIBUTIONS

Y.S. and Y.C. conceived, designed, and conducted the research; H.Z. and J.W. analyzed the data; Y.L. and J.B. drew the images; and C.H. and Z.S. supervised the research.

DECLARATION OF INTERESTS

The authors declare no competing interests.

DECLARATION OF GENERATIVE AI AND AI-ASSISTED TECHNOLOGIES IN THE WRITING PROCESS

During the preparation of this work, the authors used Large Language Model (ChatGPT 3.5). This technology was only used to improve readability and language. After using this tool, the authors reviewed and edited the content as needed and take full responsibility for the content of the publication.

Received: November 5, 2023
Revised: January 5, 2024
Accepted: February 22, 2024
Published: February 28, 2024

REFERENCES

1. Brooks, G.A. (2018). The Science and Translation of Lactate Shuttle Theory. Cell Metabol. *27*, 757–785. https://doi.org/10.1016/j.cmet.2018.03.008.
2. Kes, M.M.G., Van den Bossche, J., Griffioen, A.W., and Huijbers, E.J.M. (2020). Oncometabolites lactate and succinate drive pro-angiogenic macrophage response in tumors. Biochim. Biophys. Acta Rev. Canc *1874*, 188427. https://doi.org/10.1016/j.bbcan.2020.188427.
3. Li, X., Yang, Y., Zhang, B., Lin, X., Fu, X., An, Y., Zou, Y., Wang, J.X., Wang, Z., and Yu, T. (2022). Lactate metabolism in human health and disease. Signal Transduct. Targeted Ther. *7*, 305. https://doi.org/10.1038/s41392-022-01151-3.
4. Zhang, D., Tang, Z., Huang, H., Zhou, G., Cui, C., Weng, Y., Liu, W., Kim, S., Lee, S., Perez-Neut, M., et al. (2019). Metabolic regulation of gene expression by histone lactylation. Nature *574*, 575–580. https://doi.org/10.1038/s41586-019-1678-1.
5. Ippolito, L., Comito, G., Parri, M., Iozzo, M., Duatti, A., Virgilio, F., Lorito, N., Bacci, M., Pardella, E., Sandrini, G., et al. (2022). Lactate Rewires Lipid Metabolism and Sustains a Metabolic-Epigenetic Axis in Prostate Cancer. Cancer Res. *82*, 1267–1282. https://doi.org/10.1158/0008-5472.Can-21-0914.
6. Batlle, E., and Clevers, H. (2017). Cancer stem cells revisited. Nat. Med. *23*, 1124–1134. https://doi.org/10.1038/nm.4409.
7. Liu, S., Zhao, H., Hu, Y., Yan, C., Mi, Y., Li, X., Tao, D., and Qin, J. (2022). Lactate promotes metastasis of normoxic colorectal cancer stem cells through PGC-1α-mediated oxidative phosphorylation. Cell Death Dis. *13*, 651. https://doi.org/10.1038/s41419-022-05111-1.
8. Zhao, F., Wang, Z., Li, Z., Liu, S., and Li, S. (2022). Identifying a lactic acid metabolism-related gene signature contributes to predicting prognosis, immunotherapy efficacy, and tumor microenvironment of lung adenocarcinoma. Front. Immunol. *13*, 980508. https://doi.org/10.3389/fimmu.2022.980508.
9. Jiang, E., Xu, Z., Wang, M., Yan, T., Huang, C., Zhou, X., Liu, Q., Wang, L., Chen, Y., Wang, H., et al. (2019). Tumoral microvesicle-activated glycometabolic reprogramming in fibroblasts promotes the progression of oral squamous cell carcinoma. Faseb. J. *33*, 5690–5703. https://doi.org/10.1096/fj.201802226R.
10. Zhao, H., Jiang, E., and Shang, Z. (2020). 3D Co-culture of Cancer-Associated Fibroblast with Oral Cancer Organoids. J. Dent. Res. *100*, 201–208. https://doi.org/10.1177/0022034520956614.

11. Forlino, A., Cabral, W.A., Barnes, A.M., and Marini, J.C. (2011). New perspectives on osteogenesis imperfecta. Nat. Rev. Endocrinol. *7*, 540–557. https://doi.org/10.1038/nrendo.2011.81.
12. Cox, T.R., Bird, D., Baker, A.M., Barker, H.E., Ho, M.W.Y., Lang, G., and Erler, J.T. (2013). LOX-mediated collagen crosslinking is responsible for fibrosis-enhanced metastasis. Cancer Res. *73*, 1721–1732. https://doi.org/10.1158/0008-5472.Can-12-2233.
13. Gao, H., Chakraborty, G., Zhang, Z., Akalay, I., Gadiya, M., Gao, Y., Sinha, S., Hu, J., Jiang, C., Akram, M., et al. (2016). Multi-organ Site Metastatic Reactivation Mediated by Non-canonical Discoidin Domain Receptor 1 Signaling. Cell *166*, 47–62. https://doi.org/10.1016/j.cell.2016.06.009.
14. Wu, X., Cai, J., Zuo, Z., and Li, J. (2019). Collagen facilitates the colorectal cancer stemness and metastasis through an integrin/PI3K/AKT/Snail signaling pathway. Biomed. Pharmacother. *114*, 108708. https://doi.org/10.1016/j.biopha.2019.108708.
15. Ma, H.P., Chang, H.L., Bamodu, O.A., Yadav, V.K., Huang, T.Y., Wu, A.T.H., Yeh, C.T., Tsai, S.H., and Lee, W.H. (2019). Collagen 1A1 (COL1A1) Is a Reliable Biomarker and Putative Therapeutic Target for Hepatocellular Carcinogenesis and Metastasis. Cancers *11*, 786. https://doi.org/10.3390/cancers11060786.
16. Zhao, H., Li, R., Chen, Y., Yang, X., and Shang, Z. (2023). Stromal nicotinamide N-methyltransferase orchestrates the crosstalk between fibroblasts and tumour cells in oral squamous cell carcinoma: evidence from patient-derived assembled organoids. Oncogene *42*, 1166–1180. https://doi.org/10.1038/s41388-023-02642-5.
17. Oosterlaken, B.M., Vena, M.P., and de With, G. (2021). In Vitro Mineralization of Collagen. Adv. Mater. *33*, e2004418. https://doi.org/10.1002/adma.202004418.
18. Elia, I., Rossi, M., Stegen, S., Broekaert, D., Doglioni, G., van Gorsel, M., Boon, R., Escalona-Noguero, C., Torrekens, S., Verfaillie, C., et al. (2019). Breast cancer cells rely on environmental pyruvate to shape the metastatic niche. Nature *568*, 117–121. https://doi.org/10.1038/s41586-019-0977-x.
19. Mekhail, K., Gunaratnam, L., Bonicalzi, M.E., and Lee, S. (2004). HIF activation by pH-dependent nucleolar sequestration of VHL. Nat. Cell Biol. *6*, 642–647. https://doi.org/10.1038/ncb1144.
20. Gilkes, D.M., Chaturvedi, P., Bajpai, S., Wong, C.C., Wei, H., Pitcairn, S., Hubbi, M.E., Wirtz, D., and Semenza, G.L. (2013). Collagen prolyl hydroxylases are essential for breast cancer metastasis. Cancer Res. *73*, 3285–3296. https://doi.org/10.1158/0008-5472.CAN-12-3963.
21. Shi, R., Zhang, Z., Zhu, A., Xiong, X., Zhang, J., Xu, J., Sy, M.S., and Li, C. (2022). Targeting type I collagen for cancer treatment. Int. J. Cancer *151*, 665–683. https://doi.org/10.1002/ijc.33985.
22. Xu, S., Xu, H., Wang, W., Li, S., Li, H., Li, T., Zhang, W., Yu, X., and Liu, L. (2019). The role of collagen in cancer: from bench to bedside. J. Transl. Med. *17*, 309. https://doi.org/10.1186/s12967-019-2058-1.
23. Necula, L., Matei, L., Dragu, D., Pitica, I., Neagu, A., Bleotu, C., Diaconu, C.C., and Chivu-Economescu, M. (2022). Collagen Family as Promising Biomarkers and Therapeutic Targets in Cancer. Int. J. Mol. Sci. *23*, 12415. https://doi.org/10.3390/ijms232012415.
24. Prasetyanti, P.R., and Medema, J.P. (2017). Intra-tumor heterogeneity from a cancer stem cell perspective. Mol. Cancer *16*, 41. https://doi.org/10.1186/s12943-017-0600-4.
25. Wang, N., Jiang, X., Zhang, S., Zhu, A., Yuan, Y., Xu, H., Lei, J., and Yan, C. (2021). Structural basis of human monocarboxylate transporter 1 inhibition by anti-cancer drug candidates. Cell *184*, 370–383.e13. https://doi.org/10.1016/j.cell.2020.11.043.
26. Drent, M., Cobben, N.A., Henderson, R.F., Wouters, E.F., and van Dieijen-Visser, M. (1996). Usefulness of lactate dehydrogenase and its isoenzymes as indicators of lung damage or inflammation. Eur. Respir. J. *9*, 1736–1742. https://doi.org/10.1183/09031936.96.09081736.
27. Brown, T.P., and Ganapathy, V. (2020). Lactate/GPR81 signaling and proton motive force in cancer: Role in angiogenesis, immune escape, nutrition, and Warburg phenomenon. Pharmacol. Ther. *206*, 107451. https://doi.org/10.1016/j.pharmthera.2019.107451.
28. Majmundar, A.J., Wong, W.J., and Simon, M.C. (2010). Hypoxia-inducible factors and the response to hypoxic stress. Mol. Cell *40*, 294–309. https://doi.org/10.1016/j.molcel.2010.09.022.
29. Semenza, G.L. (2003). Targeting HIF-1 for cancer therapy. Nat. Rev. Cancer *3*, 721–732. https://doi.org/10.1038/nrc1187.
30. Gorres, K.L., and Raines, R.T. (2010). Prolyl 4-hydroxylase. Crit. Rev. Biochem. Mol. Biol. *45*, 106–124. https://doi.org/10.3109/10409231003627991.
31. Liu, L., Michowski, W., Kolodziejczyk, A., and Sicinski, P. (2019). The cell cycle in stem cell proliferation, pluripotency and differentiation. Nat. Cell Biol. *21*, 1060–1067. https://doi.org/10.1038/s41556-019-0384-4.
32. Sung, H., Ferlay, J., Siegel, R.L., Laversanne, M., Soerjomataram, I., Jemal, A., and Bray, F. (2021). Global Cancer Statistics 2020: GLOBOCAN Estimates of Incidence and Mortality Worldwide for 36 Cancers in 185 Countries. CA A Cancer J. Clin. *71*, 209–249. https://doi.org/10.3322/caac.21660.
33. Reya, T., Morrison, S.J., Clarke, M.F., and Weissman, I.L. (2001). Stem cells, cancer, and cancer stem cells. Nature *414*, 105–111. https://doi.org/10.1038/35102167.
34. Gupta, P.B., Chaffer, C.L., and Weinberg, R.A. (2009). Cancer stem cells: mirage or reality? Nat. Med. *15*, 1010–1012. https://doi.org/10.1038/nm0909-1010.
35. Yang, L., Shi, P., Zhao, G., Xu, J., Peng, W., Zhang, J., Zhang, G., Wang, X., Dong, Z., Chen, F., and Cui, H. (2020). Targeting cancer stem cell pathways for cancer therapy. Signal Transduct. Targeted Ther. *5*, 8. https://doi.org/10.1038/s41392-020-0110-5.
36. Huang, T., Song, X., Xu, D., Tiek, D., Goenka, A., Wu, B., Sastry, N., Hu, B., and Cheng, S.Y. (2020). Stem cell programs in cancer initiation, progression, and therapy resistance. Theranostics *10*, 8721–8743. https://doi.org/10.7150/thno.41648.
37. Wang, C., Li, Y., Jia, L., Kim, J.K., Li, J., Deng, P., Zhang, W., Krebsbach, P.H., and Wang, C.Y. (2021). CD276 expression enables squamous cell carcinoma stem cells to evade immune surveillance. Cell Stem Cell *28*, 1597–1613.e7. https://doi.org/10.1016/j.stem.2021.04.011.
38. Liberti, M.V., and Locasale, J.W. (2016). The Warburg Effect: How Does it Benefit Cancer Cells? Trends Biochem. Sci. *41*, 211–218. https://doi.org/10.1016/j.tibs.2015.12.001.
39. Liang, L., Li, W., Li, X., Jin, X., Liao, Q., Li, Y., and Zhou, Y. (2022). 'Reverse Warburg effect' of cancer-associated fibroblasts (Review). Int. J. Oncol. *60*, 67. https://doi.org/10.3892/ijo.2022.5357.
40. Hayashido, Y., Kitano, H., Sakaue, T., Fujii, T., Suematsu, M., Sakurai, S., and Okamoto, T. (2014). Overexpression of integrin αv facilitates proliferation and invasion of oral squamous cell carcinoma cells via MEK/ERK signaling pathway that is activated by interaction of integrin αvβ8 with type I collagen. Int. J. Oncol. *45*, 1875–1882. https://doi.org/10.3892/ijo.2014.2642.
41. Zhang, K., Corsa, C.A., Ponik, S.M., Prior, J.L., Piwnica-Worms, D., Eliceiri, K.W., Keely, P.J., and Longmore, G.D. (2013). The collagen receptor discoidin domain receptor 2 stabilizes SNAIL1 to facilitate breast cancer metastasis. Nat. Cell Biol. *15*, 677–687. https://doi.org/10.1038/ncb2743.
42. Yamazaki, S., Higuchi, Y., Ishibashi, M., Hashimoto, H., Yasunaga, M., Matsumura, Y., Tsuchihara, K., Tsuboi, M., Goto, K., Ochiai, A., and Ishii, G. (2018). Collagen type I induces EGFR-TKI resistance in EGFR-mutated cancer cells by mTOR activation through Akt-independent pathway. Cancer Sci. *109*, 2063–2073. https://doi.org/10.1111/cas.13624.
43. Huang, H., Svoboda, R.A., Lazenby, A.J., Saowapa, J., Chaika, N., Ding, K., Wheelock, M.J., and Johnson, K.R. (2016). Up-regulation of N-cadherin by Collagen I-activated Discoidin Domain Receptor 1 in Pancreatic Cancer Requires the Adaptor Molecule Shc1. J. Biol. Chem. *291*, 23208–23223. https://doi.org/10.1074/jbc.M116.740605.
44. Kirkland, S.C. (2009). Type I collagen inhibits differentiation and promotes a stem cell-like phenotype in human colorectal carcinoma cells. Br. J. Cancer *101*, 320–326. https://doi.org/10.1038/sj.bjc.6605143.
45. Ibbetson, S.J., Pyne, N.T., Pollard, A.N., Olson, M.F., and Samuel, M.S. (2013). Mechanotransduction pathways promoting tumor progression are activated in invasive human squamous cell carcinoma. Am. J. Pathol. *183*, 930–937. https://doi.org/10.1016/j.ajpath.2013.05.014.
46. Chen, W., Wang, P., Lu, Y., Jin, T., Lei, X., Liu, M., Zhuang, P., Liao, J., Lin, Z., Li, B., et al. (2019). Decreased expression of mitochondrial miR-5787 contributes to chemoresistance by reprogramming glucose metabolism and inhibiting MT-CO3 translation. Theranostics *9*, 5739–5754. https://doi.org/10.7150/thno.37556.
47. Jiang, W., Zhang, T., Zhang, H., Han, T., Ji, P., and Ou, Z. (2023). Metabolic Patterns of High-Invasive and Low-Invasive Oral Squamous Cell Carcinoma Cells Using Quantitative Metabolomics and (13)C-Glucose Tracing. Biomolecules *13*. https://doi.org/10.3390/biom13121806.
48. Chen, Y., Shao, Z., Jiang, E., Zhou, X., Wang, L., Wang, H., Luo, X., Chen, Q., Liu, K., and Shang, Z. (2020). CCL21/CCR7 interaction promotes EMT and enhances the stemness of OSCC via a JAK2/STAT3 signaling pathway. J. Cell. Physiol. *235*, 5995–6009. https://doi.org/10.1002/jcp.29525.

STAR★METHODS

KEY RESOURCES TABLE

REAGENT or RESOURCE	SOURCE	IDENTIFIER
Antibodies		
Anti-COL1A1	Cell Signaling Technology	Cat#72026; RRID:AB_2904565
Anti-P4HA1	Proteintech	Cat#12658-1-AP; RRID:AB_2283162
Anti-LDHB	Proteintech	Cat#19988-1-AP; RRID:AB_10638780
Anti-MCT1	Proteintech	Cat#20139-1-AP; RRID:AB_2878645
Anti-ALDH1A1	Proteintech	Cat#15910-1-AP; RRID:AB_2305276
Anti-Cyclin D1	Proteintech	Cat#60186-1-Ig; RRID:AB_10793718
Anti-Cyclin E1	Proteintech	Cat#11554-1-AP; RRID:AB_2071066
Anti-OCT4	Proteintech	Cat#11263-1-AP; RRID:AB_2167545
Anti-HIF-1α	Cell Signaling Technology	Cat#36169; RRID:AB_2799095
Anti-Phospho-RB	ABclonal	Cat#AP0088; RRID:AB_2771495
Anti-CD44	Proteintech	Cat#60224-1-Ig; RRID:AB_11042767
APC Anti-CD133	Biolengend	Cat#372806; RRID:AB_2632882
PE Anti-CD44	Biolengend	Cat#397503; RRID:AB_2814372
Anti-rabbit IgG HRP Conjugated	BIOPRIMACY	Cat#PMK-014-090M
Anti-mouse IgG HRP Conjugated	BIOPRIMACY	Cat#PMK-014-091M
Anti-ACTB HRP Conjugated	BIOPRIMACY	Cat#PMK058M
Goat anti-Mouse IgG, CY3	BIOPRIMACY	Cat#PMK-014-095M
Goat anti-Rabbit IgG, CY3	BIOPRIMACY	Cat#PMK-014-096M
Goat anti-Mouse IgG, FITC	BIOPRIMACY	Cat#PMK-014-093M
Goat anti-Rabbit IgG, FITC	BIOPRIMACY	Cat#PMK-014-094M
Bacterial and virus strains		
LV-GV248-COL1A1-Human	Genechem	N/A
LV-GV493-HIF-1α-Human	Genechem	N/A
LV-GV654-LDHB-Human	Genechem	N/A
pLV3-CMV-COL1A1(human)-3×FLAG-CopGFP-Puro	MiaoLingBio	N/A
pLV3-CMV-P4HA1(human)-3×FLAG-CopGFP-Puro	MiaoLingBio	N/A
Chemicals, peptides, and recombinant proteins		
AZD3965	MACKLIN	Cat#1448671-31-5
Palbociclib	MedChemExpress	Cat#HY-50767
TRIzol	Takara	Cat#Takara.9108
HiScript III RT SuperMix	Vazyme	R323-01
ChamQ SYBR	Vazyme	VQ311-02
QuickBlock™ Blocking Buffer for Western Blot	Beyotime	Cat# P0252
Super ECL	BIOPRIMACY	Cat#PMK003
B27	Gibco	Cat#17504
human EGF	PeproTech	Cat#AF-100-15
human bFGF	PeproTech	Cat#100-18B
Collagen I	Corning	Cat#356236
Tissue-Tek® O.C.T. Compound	SAKURA	Cat#4583

(*Continued on next page*)

Continued

REAGENT or RESOURCE	SOURCE	IDENTIFIER
Critical commercial assays		
α-Ketoglutarate (KG) HPLC Assay Kit	Solarbio	Cat#BC4704
Pyruvate (PA) Content Assay Kit	Solarbio	Cat#BC2205
Lactic Acid Assay kit	Nanjing Jiancheng Bioengineering Institute	Cat#A019-2-1
EdU Cell Proliferation Kit	Beyotime	Cat#C0078
Cell Cycle Analysis Kit	Beyotime	Cat#C1052
Pierce Magnetic ChIP Kit	Thermo Fisher Scientific	Cat#26157
Deposited data		
RNASeq	This paper	SRA-PRJNA1035802
Experimental models: Cell lines		
CAL-27	ATCC	CRL-2095
SCC-9	ATCC	CRL-1629
Experimental models: Organisms/strains		
BALB/c nude mice	Beijing Vital River	N/A
Oligonucleotides		
See Table S1	Sangon Biotech	N/A
Software and algorithms		
Prism 9.0 software	GraphPad	https://www.graphpad.com/
ImageJ	NIH	https://imagej.nih.gov/ij/
Image Studio	LI-COR	https://www.licor.com/bio

RESOURCE AVAILABILITY

Lead contact

Further information and requests for resources and reagents should be directed to and will be fulfilled by the lead contact, Prof. Shang (shangzhengjun@whu.edu.cn).

Materials availability

This study do not generate new unique reagents.

Data and code availability

- RNA sequencing data is publicly available through Sequence Read Archive (PRJNA1035802).
- This manuscript does not report original code.
- Any additional information required to reanalyze the data reported in this paper is available from the lead contact upon request.

EXPERIMENTAL MODEL AND STUDY PARTICIPANT DETAILS

Mouse xenografts

All animal experiments were approved by the Ethics Committee of the Hospital of Stomatology at Wuhan University (Approval number: S07922040J). 20 female BALB/c nude mice (four weeks old, Vital River, Beijing, China) were divided into group negative control (NC), lactate treatment (LAC), HIF-1αi, and LDHBi with lactate treatment (LAC+HIF-1αi+LDHBi) and Col I recovery (LAC+HIF-1αi+LDHBi+Col I) (n=5). 3×10^6 pre-infected CAL27 cells were injected subcutaneously. The above 4 groups were sequentially injected with PBS (50 μL), 3 mM lactate (50 μL), 3 mM lactate (50 μL) or 3 mM lactate with 1% exogenous Col I (50 μL) once every 4 days. 1 month later, Euthanasia was used for mice (automated CO_2 delivery systems) and the tumors were collected and measured.

Cell lines and culture

CAL27 and SCC9 cell lines were purchased from American Type Culture Collection. CAL27 cells were cultivated in DMEM. SCC9 cells were cultivated in DMEM/F-12. Both culture mediums were added with penicillin/streptomycin (ST488, Beyotime, Shanghai, China) and 10% fetal bovine serum (10099141, Gibco, Australia). Cells were cultured at 37°C in a humidified atmosphere containing 5% CO_2.

METHOD DETAILS

Sphere formation assay

5 000 cells were inoculated in ultra-low attached plates with standard CSC medium with or without 3 mM lactate. 1% exogenous Col I (356236, Corning) was added as a recovery experiment. The DMEM/F12 medium was supplemented with 2% B27 (17504, Gibco, CA, USA), 20 ng/ml human EGF (AF-100-15, PeproTech, Rocky Hill, NJ, USA), 20 ng/ml human bFGF (100-18B, PeproTech), and penicillin/streptomycin. After 10 days, photographed and counted under a microscope, then collected the spheres.

Immunofluorescence

Cells were seeded on 24-well plates containing medium with or without 3 mM lactate. Spheres were embedded in frozen cutting compound (SAKURA) and sliced at 8 μm. The plates and sections were fixed with paraformaldehyde and blocked with BSA for 1 h. The PBS was used to wash between the two steps twice. The samples were incubated with primary antibodies at 4°C overnight and washed 3 times afterward. Corresponding secondary fluorescent antibodies were used to incubate for 1 h. Antifade Mounting Medium with DAPI was added for nuclear staining after 3 times sample washing. Fluorescence microscopy (Biozero BZ-8000; Keyence, Osaka, Japan) and confocal microscopy (Andor Revolution XD, Andor Belfast, UK) were utilized to acquire images of stained samples. ImageJ was used for data analysis.

Flow cytometry

For cancer stem cell-related marker detection, CAL27 and SCC9 were seeded on 6-well dishes with or without 3 mM lactate. Cells were resuspended in a flow cytometry tube containing PBS after digestion. After centrifugation at 300 g for 5 min, the supernatant was discarded. PBS with 3% BSA was added for blocking and incubated for 30 min. After centrifugation at 300 g for 5 min, the supernatant was discarded again. APC Anti-CD133 (5 μl in 100 μl PBS) and PE Anti-CD44 (0.5 μl in 100 μl PBS) were added to the cell and resuspension. Incubation was performed in the dark on ice for 15-20 min. Cells were washed twice with 2 ml PBS. Flow cytometry analysis was then conducted. For Cell cycle analysis, Negative control and Col1A1 knockdown cells of CAL27 and SCC9 were seeded on 6-well dishes with or without 3 mM lactate. Premeasured cells were fixed in 70% ice ethanol for at least 2 h and stained with Propidium and RNase A. More details were operated according to the instruction of the Cell Cycle Analysis Kit (Beyotime), and the results were measured with Flow cytometry (BD Biosciences, San Jose, CA, USA).

EdU assay

EdU assay was used to measure the proportion of proliferating cells. HNSCCs were uniformly seeded on 24-well plates and mixed with 3 mM lactate for 48 h. An equal volume of pre-heated Edu working solution (2X, 20 μM) was added to the previous medium in the plates which were continued to place in the incubator. The plates were fixed in 2 h and stained using the EdU Cell Proliferation Kit (C0078, Beyotime) as instructed. Cells were observed and photographed under a fluorescence microscope (Biozero BZ-8000, Keyence, Osaka, Japan).

Western blot

The membranes were handled with the primary antibodies for 4°C overnight incubation after being blocked with QuickBlock™ Blocking Buffer for 20 min. The dilution of corresponding secondary antibodies were used to treat protein membranes for 1 h. Then ECL kit was used to display the results. Protein membranes were washed by TBST three times between every step. Images were acquired and analyzed using Image Studio software. The antibodies used were provided in key resources table.

Lactate uptake and pyruvate (PA) detection

10 000 cells were inoculated in ultra-low attached plates (3741, Corning) with standard CSC medium with or without 3 mM lactate to measure lactate and PA metabolism of HNSCC cells. The supernatant and cells were collected every 12 h. At the same time, the cells' densities were measured to correct the final results. The extracellular lactate concentration in the supernatants and the intracellular PA content were evaluated according to the manufacturer's instructions of the Lactate Acid Test Kit (A019-2-1, Jiancheng, Nanjing, China) and the PA Content Assay Kit (BC2205, Solarbio, Beijing, China). Additionally, we evaluated the intracellular levels of lactate and PA 48 h after negative/lactate treatment in the NC, LAC, siMCT1+LAC, and siLDHB+LAC groups.

Colony formation assay

200 cells were implanted in each well of the 12-well plate and incubated for 10 days with or without 3 mM lactate. Fresh medium with or without 3mM lactate was changed every 3 days. 4% paraformaldehyde fix solution was used to deal with the colonies for 20 minutes, and then the plates were stained with crystal violet for 10 minutes. Wash and dry the cell mass before observing it under the microscope (Olympus, Tokyo, Japan).

Chromatin immunoprecipitation (ChIP)

For ChIP assay at least 4×10^6 cells were collected. Chromatin was cross-linked by 1% formaldehyde and the reaction was terminated by glycine solution. Membrane extraction buffer, MNase, and S220 focused-ultrasonicator (Covaris, Woburn, MA, USA) were exerted to

fragment the crosslinked chromatin. The resulting chromatin fragments were incubated with a diluted HIF-1α primary antibody or IgG in IP dilution buffer at 4°C overnight. ChIP Grade Protein A/G Magnetic Beads were exploited to attain chromatin fragments with specific binding sites. The chromatin fragments were eluted, reversed, and the specific DNA was identified by qPCR assay after recovery and purification. The detailed steps of these processes were instructed by the Pierce Magnetic ChIP Kit (26157, Thermo Fisher Scientific). The primers for 4 regions of the P4HA1 promoter were listed in Table S2.

Real-time PCR

Cells were dealt with TRIzol to procure total RNA that was reverse-transcribed to cDNA by HiScript III RT SuperMix (R323-01, Vazyme). CDNA, ChamQ SYBR (VQ311-02, Vazyme), and specific primers were included in the loading mixture. RT-PCR was operated in the Quant-Studio 6 Flex qPCR System. Changes of the mRNA expression were evaluated according to the Ct results. The primer sequences used are labeled in Table S4.

SiRNAs transfection and lentivirus infection

The experiments proceeded as previously described.[48] The siRNAs targeting HIF-1α, P4HA1, MCT1, and LDHB were designed and purchased from Hanbio (Shanghai, China). Non-influential sequences were assembled as negative control (siNC). The corresponding knockdown efficiency of siRNA was presented in Figures S2D, S2E, S3C, and S3D. The recombinant lentivirus HIF-1αi and LDHBi were constructed by GeneChem according to sequences of siHIF-1α#1 and siLDHB #1 that verified to be valid (Shanghai, China). The shCol1A1 lentivirus were purchased from GeneChem (GCD0297789), and the verification results were shown in Figure S1D. The oeCOL1A1 and oeP4HA1 was obtained from MiaoLingBio (Wuhan, China) and the verification results were shown in Figures S1E and S3A. The details of the interference sequences were described in Tables S1 and S3.

Transcriptome sequencing

The data of NC and COL1A1i group (both treated with lactate) with 3 replicates of CAL27 cells were provided by Novogene Co., Ltd (Beijing, China). Experiments were performed and results were reported in 1 month.

QUANTIFICATION AND STATISTICAL ANALYSIS

Quantification analysis of experimental data was performed using GraphPad Prism 9. Student's t-test was employed when analyzing data with only two groups, whereas One-Way ANOVA was utilized for data with three or more groups. Differences with P-values < 0.05 were considered statistically significant (*$P < 0.05$, **$P < 0.01$, ***$P < 0.001$, ****$P < 0.0001$).